UNIVERSITY OF WASHINGTON
DEPARTMENT OF
OCEANOGRAPHY

Technical Report No. 85

A MODEL STUDY OF THE STEADY-STATE SALINITY DISTRIBUTION IN PUGET SOUND

by

Harlow G. Farmer and M. Rattray, Jr.

National Science Foundation
Grant No. G15728 and G19788
and
Office of Naval Research
Contract Nonr-477(10)
Project NR 083 012

Reference M62-29
February 1963

SEATTLE 5, WASHINGTON

UNIVERSITY OF WASHINGTON
DEPARTMENT OF OCEANOGRAPHY
Seattle 5, Washington

Technical Report No. 85

A MODEL STUDY OF THE STEADY-STATE SALINITY DISTRIBUTION IN PUGET SOUND

by

Harlow G. Farmer and M. Rattray, Jr.

National Science Foundation,
Grants No. G 15728 and G 19788

Office of Naval Research,
Contract Nonr-477(10)
Project NR 083 012

Ref. M62-29
September 1962

RICHARD H. FLEMING
Chairman

TABLE OF CONTENTS

LIST OF TABLES

LIST OF FIGURES

ABSTRACT

The steady-state salinity distribution in Puget Sound has been obtained, using an oceanographic model. Seven stations which were located in the several main divisions of Puget Sound were selected and salinity profiles were obtained, at each, for three conditions of fresh water runoff and for five values of tidal range. Low monthly, annual, and high monthly mean values of runoff were used, with limits of the tidal range exceeding those generally observed in Puget Sound.

The salinity at all stations in Puget Sound is observed to be strongly dependent on the characteristics of the tidal flow in Admiralty Inlet. The shape of the salinity profile at a station is also observed to be constant for constant values of a quantity representative of the ratio of tidal flow to total runoff. Certain other features of the circulation are deduced.

The data are reproduced in Tables 2 to 8 of this report.

INTRODUCTION

Puget Sound is the only fiord-like estuary presently under study by a United States oceanographic institution. Its deep basins, strong tides, numerous arms, and the large and variable river runoff present a complex of problems of considerable oceanographic interest. As an aid in a long range program of research on Puget Sound, a small-scale model of the complete system was constructed in 1950. The model has proved most useful in the interpretation of field observations and in studies of the mechanism of circulation under controlled conditions. The construction, instrumentation and verification of the model has been reported by Barnes and Lincoln (1952), Barnes et al. (1954) and Rattray and Lincoln (1955).

The variable conditions of runoff and tide maintain Puget Sound in a continually changing state. The problems in seeking an understanding of the processes in such a large system from field or model observations are difficult. It is desirable therefore to first make a model study of the steady-state salinity distribution and circulation in the system. Subsequently, the more natural conditions of variable runoff and tide may be introduced into the model and the significance of the departures from the steady state may then be examined.

This report deals with the steady-state salinity distribution. Quantitative estimates of the several processes present which control the general circulation cannot be made from this information only. However, the salinity distribution will indicate the relative response of the different sections of the system to changes in tide and runoff and demonstrate the importance and influence of the major topographic features. This information is required for subsequent studies on the mechanisms of the circulation and will be helpful in better defining specific problems.

DESCRIPTION OF AREA AND STATION SITES

Puget Sound (Figure 1) may be divided into five clearly defined sections. Admiralty Inlet averages 40 fathoms in depth and forms the primary juncture of the system with the Strait of Juan de Fuca. The main basin, in which the depth commonly exceeds 100 fathoms, extends from the southern end of Admiralty Inlet, south to the Tacoma Narrows, a 26-fathom sill. The southern basin, which joins with the Narrows, deepens to 90 fathoms and is composed of numerous large and small inlets and islands. The northern section extends from Possession Sound, north to Deception Pass, a narrow shallow passage with high tidal currents connecting with the Strait of Juan de Fuca. The last main section is the Hood Canal which branches from the southern end of Admiralty Inlet. It deepens to 90 fathoms in its inner section from a 30- to 40-fathom entrance channel.

The thirteen largest rivers discharging into Puget Sound contribute close to 80 percent of the total fresh-water inflow. The three rivers entering the northern section alone contribute over 60 percent. In contrast, the four small rivers entering Hood Canal contribute only about 6 percent. The rivers peak and flood at different times of the year depending on their source. For example, the Nisqually River which enters the southern basin is fed by glacier and snow melt. It peaks in late spring and early summer. The rivers entering the northern section peak and flood during the rainy winter season.

Puget Sound tides are of the mixed type with ranges which progressively increase from Admiralty Inlet to the inner regions of Puget Sound. Port Townsend has a mean diurnal tide of 8 feet, Seattle, 11 feet and Olympia, 14 feet.

Seven stations were selected at which salinity profiles were taken. These are listed below and are indicated in Figure 1. The approximate depth and shore-to-shore width of the channel in the immediate vicinity of the station are given.

(1) Bush Point-- in the central part of Admiralty Inlet. The tidal currents here are in the order of 3 to 4 knots and, with the very irregular bottom topography, strong, turbulent mixing occurs. In the model no rivers discharge directly into Admiralty Inlet. Except for the relatively small flow through Deception Pass, all fresh water entering the system must flow past Bush Point before eventual dispersion in the Strait of Juan de Fuca. The depth is 60 fathoms and width 2.5 nautical miles.

(2) Camano Head-- between Whidbey Island and the southern end of Camano Island in the north section. The depth is 95 fathoms and width 1.4 nautical miles.

(3) Point Jefferson-- near the north end of the main basin. The depth is 150 fathoms and width 3.5 nautical miles.

(4) Point Pully-- in East Passage, east of Vashon Island in the southern end of the main basin. In East Passage there are both ebb and flood currents with a net clockwise circulation around Vashon Island. The depth is 110 fathoms and width is 2.3 nautical miles.

(5) Spring Beach-- near the south end of Colvos Passage, west of Vashon Island. During flood tide the currents in Colvos Passage are weak and variable.

The ebb current is strong and is dominated by the ebb flow from the Narrows. The depth is 50 fathoms and width 1.0 nautical mile.

(6) Gordon Point-- southeast of McNeil Island in the southern basin. The depth is 85 fathoms and width is about 2.2 nautical miles.

(7) Hazel Point-- in the Hood Canal at the south end of Toandos Peninsula. The depth is 50 fathoms and width 1.0 nautical miles. Extending north to Admiralty Inlet the channel depth varies between 25 and 50 fathoms and, for a distance of 5 miles, the average sill depth is approximately 30 fathoms. To the south it gradually deepens to 90 fathoms and remains between 80 and 90 fathoms for most of its length.

THE PUGET SOUND MODEL

A description of the model and its operating characteristics have already been reported and only a brief summary will be presented here. The model was constructed according to Froude scaling laws with a horizontal length scale of 1:40,000 and a vertical distortion of 34.6:1. These scale ratios permit the Reynolds number in the model to be sufficiently high that turbulence exists in nearly all regions of the model. Only in the upper reaches of the small bays and inlets does the water appear to be nonturbulent and the flow in these areas is unimportant to the main circulation. The Reynolds numbers at Bush Point and Point Jefferson in the prototype are 10^8. In the model the Reynolds numbers are approximately 2,600 and 800 respectively. The topography of Puget Sound consists of shallow sills and deep basins, narrow and broad channels, islands and a generally rough boundary. These features coupled with the tidal currents produce large and small eddies which are readily demonstrated in the model through the dispersal of small drops of miscible dye.

A criterion for turbulence in a fluid with density gradient is the Richardson number. With Froude scales for velocity and length, the salinity (density) scale must be unity for equal values of this number in model and prototype. A reduction in the salinity scale reduces the Richardson number and turbulence would be expected to increase. From the results of previous experiments it was found that the salinity structure throughout the model differed little with moderate changes in the salinity scale. A salinity scale of 1:2 has been used in the experiments reported herein.

The tide generator is controlled from a six-component tide computer. Tides from any one constituent or combination of constituents may be generated in the model. The river discharges are gauged with small precision flow meters. At each river outlet, turbulence is introduced by a small spinning shaft to provide the initial mixing of the fresh and salt water. The ocean salinity is monitored by continuous conductivity measurements and controlled automatically by introducing concentrated salt solution as needed.

DIMENSIONAL ANALYSIS

Theoretical solutions to the equations of motion that are applicable to estuarine flow are very limited in number. Those that have been obtained either have limited application, due to the idealized conditions assumed, or, through consideration of the mean motion, do not explicitly include the tidal height and period which are fundamental variables in the model study.

The salinity, S, in geometrically similar systems is assumed to be a function of a reference salinity, S_o, the total river discharge, R, entering the system, the tidal height, ζ, the tidal period, T, the channel depth, D, and width, W, the horizontal length of the system, L, the location of the observation given by the coordinates, X, Y, Z, the kinematic viscosity, ν, the density, ρ, and the acceleration due to gravity, g. The velocity of flow has not been included for it is primarily due to the tides and is a function of the tidal height and period and the geometry of the estuary. The following functional equation may be stated.

$$S = f\ [S_o,\ R,\ \zeta,\ T,\ D,\ W,\ L,\ X,\ Y,\ Z,\ \nu,\ \rho,\ g\ ]$$

From the Buckingham Pi Theorem the equation can be rewritten as:

$$\frac{S}{S_o} = f\left[\frac{X}{D}, \frac{Y}{D}, \frac{Z}{D}, \frac{\zeta}{D}, \frac{W}{D}, \frac{L}{D}, \frac{\zeta DW}{TR}, \frac{R^2}{gD^3W^2}, \mathrm{Re}, \mathrm{Ri}\right]$$

where the Reynolds and Richardson numbers are respectively, $\mathrm{Re} = \frac{\zeta D}{\nu T}$, $\mathrm{Ri} = \frac{gDT^2 S_o}{\rho\zeta^2}\frac{\partial\rho}{\partial S}$.

The highly irregular topography of Puget Sound would actually require for description the use of many more characteristic lengths and their corresponding dimensionless ratios. However, as long as the modelling is restricted to geometrically similar systems, these ratios will remain constant and they need not be included in the above expression for S. Previous experiments have shown that within the ranges of Reynolds and Richardson numbers used in this study, the ratios have no direct effect on the salinity distribution. The following two quantities are designated by the letters M and F, where M is representative of the ratio of tidal flow to river discharge, and F is a Froude number characterizing the net flows.

$$M = \frac{\zeta DW}{TR}, \qquad F = \frac{R}{\sqrt{gD^3W^2}}$$

At a particular station, the salinity dependence may be stated in the following form:

$$\frac{S}{S_o} = f\left[\frac{Z}{D}, \frac{\zeta}{D}, M, F\right]$$

As D and W are unspecified depth and width measurements, they will be chosen so that they have a value of unity for the model experiments.

EXPERIMENTAL PROCEDURE

The three parameters which are varied in the model experiments are the river discharge, R, the tidal height, ζ, and the tidal period, T.

Three states of river discharge were selected: 1) the annual mean, 2) the high monthly mean and 3) the low monthly mean. These data were obtained from the water supply papers of the U. S. Geological Survey. The gauged flow of the rivers has been increased by 25 percent to account for the ungauged small rivers and streams and direct precipitation. For the total river discharge the ratios of the high monthly and low monthly mean to the annual mean are 1.69 and 0.37 respectively. It should be noted that these ratios for the individual rivers will deviate slightly from the above average values since the seasonal cycles of the various river discharges differ.

The model was operated with the single M_2 constituent tide to facilitate defining the tidal period and the tidal height. The range of tidal amplitudes at Seattle varied between 1.22 meters and 6.30 meters.

The vertical salinity profile at each station was determined by titration of small water samples obtained at discrete depths. At the deeper stations six depths were selected, the surface, 10, 25, 50, 75 and 150 meters. At the shallower stations the surface, 25 and 100 meter depths were initially selected and later on in the course of the experiments the ten meter depth was included. A larger number of depths would have given a better approximation to the salinity profile, however, at this stage of the investigation, it was felt unjustified to spend the time required for additional titration. Details of the microtitration and sampling are given in the Appendix. In summary, 2-ml samples were withdrawn at each depth over one tidal cycle. One ml was used for rinsing and one ml was titrated using silver nitrate solution and a fluorescein indicator. Using solutions with salinities determined by standard analytical procedures, tests indicated that the microtitration procedure gave salinities with a standard deviation of 0.04 °/oo.

Temperature was determined at three or four depths using a bead type thermistor. The model was operated for a minimum of one day and frequently two to three days prior to sampling to insure that a steady-state salinity distribution had been obtained. A run included two sets of samples at each station with approximately four hours lapsing between them.

It was evident from the temperature measurements at each station that vertical and horizontal temperature gradients existed in the model and that this temperature field varied with the different runs. The maximum temperature difference between surface and bottom was approximately 1°C and maximum horizontal differences ranged up to 2° to 3°C. In several of the runs the temperature gradients were small, the maximum differences not exceeding 0.1°C. In the analysis of the salinity distributions, inconsistencies in the data could be correlated to the temperature field and its changes. When in selected cases the temperature effect was removed, these inconsistencies were effectively removed. It was decided,

therefore, to correct all the data and refer it to a single value of temperature.

The water density was computed from the measured salinity and temperature and the equation: $\rho = \rho' + \alpha S + \beta T$. This equation is suitable for a wide range of salinities if the temperature range is limited to about 5°C, as in the case of these experiments. The constants α and β have been determined using values of ρ, S, T for sea water.

$$\beta = -0.000268 \ \frac{\text{gms}}{\text{cm}^3 \text{°C}}$$

$$\alpha = 0.000760 \ \frac{\text{Kgm}}{\text{cm}^3}$$

$$\rho' = 1.00365 \ \frac{\text{gms}}{\text{cm}^3}$$

The applicable range is 21°C to 26°C and salinity is entered in parts per thousand, i.e. grams salt per kilogram solution.

With the calculated value of density and a reference temperature of 23°C, corrected salinities were calculated. The data in the Appendix are given in the two ratios $\frac{S_o - S_b}{S_o}$ and $\frac{S_b - S_z}{S_o}$. S_o is the ocean or source salinity and was, on the average, 16.50 °/oo. S_z is the salinity at depth z and S_b is the salinity at the bottom depth z_b. The standard deviation, σ, of a ratio such as $\frac{S_1 - S_2}{S_o}$, due to the known standard deviation of the salinity titrations, 0.04 °/oo, and an estimated standard deviation of the temperature measurements, 0.07°C, is $\sigma = \pm 0.004$.

EXPERIMENTAL RESULTS

Table 1 lists the tidal height, river discharge and the quantities M and F for each run. The normalized ratios $\frac{S_o - S_b}{S_o}$ and $\frac{S_b - S_z}{S_o}$ are used to describe the horizontal and vertical distributions of salinity as functions of the variables ζ, T and R. S_b was selected rather than surface S as it was anticipated that S_b would be easier to measure and would be less subject to the location of the rivers than the surface salinity. For the vertical distribution of salinity, only the shape of the distribution is emphasized by the ratio $\frac{S_b - S_z}{S_o}$. The sum of these two ratios gives the salinity at any depth in reference to that of the ocean.

The values of $\frac{S_o - S_b}{S_o}$ at each station, when plotted against, M formed three distinct curves, one curve for each state of the river discharge, R, or the Froude number F. In contrast, the bottom-surface salinity difference, $\frac{S_b - S_s}{S_o}$, and in general, $\frac{S_b - S_z}{S_o}$, does not exhibit this parametric dependence on F. This has suggested

that the salinity profiles for each station could be presented in a unified manner by plotting the salinity ratio $\frac{S_b - S_z}{S_o}$ for each of the measured depths against the quantity M. The shape of the salinity profile and the manner in which it changes is indicated by the position and relative spacing of the constant depth curves, $\frac{z}{z_b}$. These curves for each of the seven stations are presented in Figure 2a-2g. To avoid a dense array of data points, the twenty runs have been divided into five groups and the mean value of M and $\frac{S_b - S_z}{S_o}$ has been plotted. The five groups of runs are as follows:

Group	Run
1	8, 15, 17
2	2, 7, 10, 12, 24
3	1, 5, 14, 19, 21, 22
4	4, 18, 23
5	3, 6, 9

The curves of $\frac{S_o - S_b}{S_o}$ for each of the three Froude numbers, F, have been plotted in the same figure. The Froude numbers, F_1, F_2, F_3, refer to the three states of river discharge, low, mean and high respectively. A characteristic feature of these curves is that $\frac{S_o - S_b}{S_o}$ generally has a well defined maximum for each value of F. This will be discussed later in terms of the tidal flow and possible mixing mechanisms.

It will be evident from Figure 2 that some artistic license has been exercised in drawing the constant depth curves. With the exception of the Camano Head Station, the surface curves have been drawn as straight lines. This is clearly an approximation since it is to be expected that $\frac{S_b - S_s}{S_o}$ will approach unity as M approaches zero. For the larger values of M the salinity differences become small for all depths and the magnitude of $\frac{S_b - S_z}{S_o}$ is the same as the variability of the data, $\sigma = 0.004$. The consistency of the data for several of the stations is considered very good, while for others the data points are rather widely scattered. A comparison between the salinity profiles reconstructed from the $\frac{z}{z_b}$ curves and those obtained from the original data is shown in Figure 3a-3c. The shape of the salinity profiles is adequately reproduced within the limits of the experimental observations.

The shape of the salinity profiles will change as the tidal height, tidal period and river discharge are varied. If, however, these variables are allowed to change in such a way that the ratio M is constant, then, though the salinity profile may change, it will remain similar in shape. The shape of the salinity profile for several values of M and for five of the seven stations is shown in Figure 4, in which the normalized coordinate $\frac{S_b - S_z}{S_b - S_s}$ is used. The variability of this ratio is appreciably greater than the $\sigma = \pm 0.004$, as the denominator here is a salinity difference. The magnitude of σ increases as $S_b - S_s$ decreases. In Figure 4 approximate values of σ for M equal to 0.32 and 2.0 are $\pm$ 0.01 and $\pm$ 0.20 respectively. The 45^o lines in Figure 4 represent the limiting salinity

profile as the water column approaches homogeneity. This condition is approached for the larger values of M. With decreasing M, the salinity gradients increase and, as is evident in the figure, the relative shape of the profile is dependent on local effects. The reverse curvature in the curves for Point Pully indicates a tendency toward multiple stratification. Referring to the salinity profiles for Point Pully in Figure 3c, some mid-depth stratification is clearly evident near M = 0.6, while it is only weakly evident at M = 1.0. In the latter case the variability of the data could obscure this stratification, whereas near M = 0.6 it would not.

Figure 5 shows the bottom salinity ratio $\frac{S_o - S_b}{S_o}$ for all stations grouped according to Froude number, F_1, F_2, and F_3. The ordinate in the figures is the product, MF, which depends only on the variables, tidal height and tidal period. These figures clearly show the general decrease in bottom salinity S_b with increasing distance from the ocean source. The relative decrease between the various stations more strongly reflects the intervening topography and local effects than the distance between the stations. For the low tidal velocities, MF = 0.2, the bottom salinity, S_b, is observed to decrease slightly and then to increase as the river discharge is increased. These changes are not large and fall nearly within the variability of the data. At higher tidal velocities the bottom salinity decreases consistently with increasing river discharge. A result of using the ordinate MF is that the maximum value of the bottom salinity ratio occurs at approximately MF = 0.5 for all river discharges and all stations with the exception of Hazel Point. The maximum $\frac{S_o - S_b}{S_o}$ for Hazel Point occurs at MF = 0.7.

DISCUSSION OF EXPERIMENTAL RESULTS

There are two features of particular interest indicated in the data. The first is the observed change in bottom salinity with tidal velocity. For a constant state of river discharge and with increasing tidal velocity, the bottom salinity initially decreases, passes through a minimum value and then increases. Figure 2 shows that the whole water column changes in salinity in the same sense as the bottom salinity, and, with increasing tidal velocity, the salinity changes less with depth. Figure 5 shows further that this minimum bottom salinity occurs at approximately the same value of tidal velocity for all stations, with the exception of that at Hazel Point which is located near the north end of the Hood Canal. The second feature of interest in the results is the similarity of the salinity profiles for constant values of M, the ratio of tidal flow to river discharge. These results will be discussed briefly in reference to theoretical models of estuarine circulation and to specific features of the tidal flow in Puget Sound.

The type of circulation may be directly inferred from the salinity distribution in two, clearly defined and seldom observed situations. When the water column is completely mixed in the vertical direction and only a horizontal salinity gradient exists, the horizontal transport of salt by advection must be balanced by horizontal diffusion. The other case is that of completely stratified flow when fresh water overlies the saline ocean water. Most cases of interest will lie between these limits, and knowledge of only the salinity

distribution will be insufficient to define clearly the circulation. Miscible dye solutions may be used in the model to demonstrate major features of the circulation. During these experiments the dye solutions were used sparingly, since frequent use quickly contaminated and dirtied the model. These experiments and those performed previously have shown a general movement upstream in the deeper, more saline water and a net downstream flow in the upper layers. Particular current systems such as the net circulation around Vashon Island have been clearly demonstrated.

The flux of salt by vertical and horizontal advection and vertical and horizontal diffusion have been calculated by Pritchard (1954) for the James River, a coastal plain estuary, and by McAlister, et al. (1959) for Silver Bay, Alaska, a fiord type estuary. Pritchard has found that horizontal advection and vertical diffusion predominate, vertical advection is of lesser importance and horizontal diffusion of little significance. McAlister finds horizontal and vertical advection to be predominant, and vertical and horizontal diffusion both small to insignificant. From these two analyses the main difference in transport mechanisms between the coastal and fiord type estuary is in the relative magnitude of vertical diffusion and vertical advection. The bathymetry of Puget Sound has features similar to those of a fiord but has a salinity distribution more like that of the coastal plain estuary. Analyses similar to those of Pritchard and McAlister have not as yet been made for Puget Sound. The main observed changes in salinity of this system can be explained, however, through a consideration of the tidal flow in Admiralty Inlet, Hood Canal and the Tacoma Narrows.

Admiralty Inlet is a relatively shallow channel, connecting deeper basins. The salt transport by the tidal flow through this channel will be significantly influenced by the tidal range. The length of Admiralty Inlet, extending from Double Bluff, just south of the Hood Canal entrance to the Strait of Juan de Fuca, is 18 miles. At the entrance to Admiralty Inlet there is a small sill extending for two miles with 40 meters depth of water over it. Along the remaining 16 miles, the depth averages 80 meters, and south of Double Bluff, the depth increases to 200 meters in a distance of 4 miles. For a tidal range of 3.5 meters at Seattle, the tidal excursion in Admiralty Inlet is 17 miles, the approximate length of the sill. When tides exceed this mean tidal condition, the more saline water from the Strait of Juan de Fuca will pass completely through Admiralty Inlet and enter the main basin of Puget Sound in one flood tide. For lower tidal ranges, the waters from the Strait will require more than one tidal cycle to reach the inner basin and during the intervening ebb and flood flows it will experience more mixing and dilution with the fresher surface water.

This tidal flow over the entrance sill acts as a control on the salinity of the water available to the interior basins. With low tidal ranges, it is predominantly the tidal velocity which provides the turbulent mixing processes over the sill that controls the salinity of the entering water. When the tidal excursion exceeds the length of the sill, the salinity of the entering water depends more on the tidal height than the tidal velocity.

A similar situation appears to exist in the northern section of Hood Canal. From Hazel Point at the south end to Tala Point, at its juncture with Admiralty Inlet, this section is 17 miles long. In the central five miles there is a

fairly well defined sill over which the depth of water is approximately 55 meters. To the north and south the depth increases gradually at first and then more rapidly to about 100 meters, and south of Hazel Point, the depth increases to 180 meters. For the 3.5 meter tide at Seattle the tidal excursion over this central sill is approximately 4 miles. With this tidal range the more saline bottom waters from Admiralty Inlet will require more than one tidal cycle to pass over the sill to the inner basin. A 30 percent increase in the tidal range will increase the tidal excursion to the approximate length of the sill. This increase in tidal range would appear to explain why the observed bottom salinity at Hazel Point reaches its minimum (Fig. 5) at a value of MF, about 30 percent greater than that for all the other stations.

The bottom salinity at Gordon Point which lies south of the Tacoma Narrows in Southern Puget Sound follows, essentially, the salinity of the main basin to the north. As only a tide of about 0.7 meters at Seattle is required for the tidal excursion and sill length to be equal in the Narrows, in all the experimental observations the waters in the main basin pass completely through the Narrows in each tidal cycle.

In the range of M = 0.5 to 0.7 the salinity profile at Point Pully indicates a tendency towards stratification with an upper layer of 50 to 75 meters depth. This development of two layers is attributed to the influence of the ebb flow from Colvos Passage and the net circulation around Vashon Island. With these conditions, the ebb flow from Colvos Passage is less saline than water at the same depth in the main basin. On the following flood tide, part of the water in the upper layer of the main basin, freshened by mixing with the water from Colvos Passage, returns to the south through East Passage. For M less than 0.5 and greater than 0.7 the salinity of the ebb flow from Colvos Passage, as indicated by that at Spring Beach, more nearly approximates the salinity in the main basin and a less noticeable effect results from the mixing of the waters.

It is also apparent from Figure 4 that for the higher values of M, the salinity at Point Pully tends to be nearly constant over the depth for a greater range of the parameter M than does the salinity at any of the other stations. This results, during the higher tidal ranges, from the waters of East Passage, the Puyallup River and the southern basin being thoroughly mixed by the strong tidal currents in the Narrows and Colvos Passage. The runoff of the Duwamish and Cedar Rivers which enter north of Alki Point flow predominantly to the north and have little influence on the salinity in East Passage.

The greatest range in shape of the salinity profile is found at Point Jefferson. This results from the influence of the fresh water from the three large rivers to the north which, in passing around the southern end of Whidbey Island, penetrate progressively further to the south into the main basin as the runoff increases. In the vicinity of the Camano Head Station, the water is strongly stratified in a shallow surface layer, but after it has passed into the north end of the main basin the turbulence from the stronger tidal currents rapidly mixes the water and establishes weaker salinity gradients.

The model results show that the relative shapes of the salinity profiles are constant for a constant value of the parameter M. The several profiles, shown in Figure 4 for each of the stations, with the exception of Point Pully, exhibit some similarity to each other, suggesting the existence of a similarity

coordinate for the salinity, as was obtained theoretically by Rattray and Hansen (1962).

The differences and changes in the salinity structure in the several regions of Puget Sound are however more clearly evident in Figure 2. The constant depth lines for the Bush Point, Hazel Point, Gordon Point, and Spring Beach stations are either straight or only slightly curved lines, and would indicate similar type salinity profiles. In contrast, the constant depth lines for Point Jefferson and Pully Point which lie in the main basin and Camano Head, immediately adjoining it, are far more complex. The minimums in the constant depth curves for the intermediate layers of the main basin reflect some influence of the deep water, but at Camano Head this effect is less pronounced.

CONCLUSIONS

(a) The steady-state salinity distribution was obtained for a semi-diurnal tide ranging from 2.44 meters to 6.30 meters at Seattle, and for the low monthly mean, annual mean, and high monthly mean river discharges.

(b) The shape of the salinity profile at a particular station remained constant for a constant value of M, the ratio of tidal flow to total river discharge, but differed with the location of the station.

(c) The bottom salinity of the profile at each station effectively indicates the trend of the salinity of the water column in response to changing tidal and runoff conditions and demonstrates the transport of fresh water to all depths.

(d) The mean salinity of all stations is strongly influenced by changes in tidal height and velocity in Admiralty Inlet. The station in Hood Canal is further influenced by the tidal height and velocity over the sill-like structure in its entrance channel. The general response at constant river discharge is that for less than average tide conditions, the mean salinity decreases for increasing tide, while for greater than average tide conditions the mean salinity increases with increasing tide.

(e) The microtitration technique proved satisfactory and with average care was accurate to $\pm$ 0.04 °/oo.

Barnes, C. A., and J. H. Lincoln
1952. An Hydraulic tidal model of the Puget Sound area. Trans. Amer. Geo. Union, v. 33, p. 323.

Barnes, C. A., J. H. Lincoln and M. Rattray, Jr.
1957. An oceanographic model of Puget Sound. Proc. VIII, Pacific Science Congress, v. 3, pp. 686-704.

Lincoln, J. H., R. G. Paquette and M. Rattray, Jr.
1955. Microsalinometer for oceanographic model studies. Trans. Am. Geo. Union, v. 36, no. 3, pp. 406-412.

McAlister, W. B., M. Rattray, Jr. and C. A. Barnes
1959. The dynamics of a fiord estuary: Silver Bay, Alaska. Univ. of Wash. Dept. of Oceanography, Tech. Rept. no. 62, Ref. 59-28, 70 pp.

Pritchard, D. W.
1954. A study of the salt balance in a central plain estuary. Jour. Mar. Res., v. 13, no. 1, pp. 133-144.

Rattray, M. Jr. and J. H. Lincoln
1955. Operating characteristics of an oceanographic model of Puget Sound. Trans. Amer. Geo. Union, v. 36, no. 2, pp. 251-261.

Rattray, M., Jr. and D. V. Hansen
1962. A similarity solution for circulation in an estuary. Jour. Mar. Res., v. 20, no. 2, pp. 121-133.

APPENDIX

Microtitration Procedure

The water samples to be withdrawn from the model for salinity determination necessarily had to be small to avoid disturbing the salinity distribution. The 15-ml sample required for the standard Knudsen titration procedure was far too large even without consideration of the larger sample needed to provide for rinsing. The following procedure was established, which required only a 1-ml sample for titration. It met the accuracy requirement of at least 0.05 °/oo and needed a minimum amount of time and care.

The samplers permitted withdrawal of water from a total of six preselected depths at one time. Small-diameter Monel tubes were inserted to the desired depths and at the other ends, pierced rubber stoppers were placed over the tubes and glass vials were attached. A 50-to 60-mm Hg vacuum applied to the vials withdrew about 2 ml of water uniformly over a tidal cycle. The six tubes and rubber stoppers were mounted on a frame and the vacuum connections were permanently made through each stopper. The frame could be easily placed at the various stations and the glass vials, as needed, were pressed on to the rubber stoppers.

The samples were taken from the vials with a 1-cc syringe. Before filling, the syringe was rinsed three times. The syringe was mounted on a frame and a stop was provided for the plunger so that a constant volume sample was obtained each time.

The samples are titrated with a silver nitrate solution and indicator solution consisting of fluorescein disodium salt and starch in distilled water. The reaction is $NaCl + AgNO_3 \rightarrow AgCl + NaNO_3$; 2.9066 grams of $AgNO_3$ are required for each gram of NaCl. The concentration of $AgNO_3$ solution was generally 37.11 grams per liter solution. Six drops of indicator solution were used in each 1-ml sample. The $AgNO_3$ solution was dispensed from a 5-cc syringe with a hollow glass needle which was kept in the stirred solution. The plunger displacement was measured by a micrometer movement. The plunger travel, L, between the positions at the beginning and at the end point is directly proportional to the salinity. This supposes constant temperature at all times, a perfectly cylindrical syringe, etc. Thus $S = KL$. K is obtained through calibration by titrating a standard solution of accurately known salinity. The micrometer and 5-cc syringe are rigidly mounted on a frame which may be raised and lowered by a rack and pinion. The constant, K, was determined each day that titrations were made. K was observed to decrease slightly with aging of the silver nitrate solution. The silver nitrate solution was renewed approximately each month.

Numerous sources of error influence the accuracy of the salinity determination. These will not be enumerated and with the exception of the micrometer setting their effects are included in the coefficient K. The standard deviation of the salinities depends therefore on the accuracy of the determination of K. The standard deviation of S is obtained by differentiating the above formula for S, squaring and taking the mean value. The differentials of K and L are assumed uncorrelated and approximating the mean square of the differentials by the variance σ^2 there is obtained

$$\left(\frac{\sigma_S}{S}\right)^2 = \left(\frac{\sigma_K}{K}\right)^2 + \left(\frac{\sigma_L}{L}\right)^2$$

The variance of K can be similarly determined from the values for S', L', σ_S', σ_L' obtained from the titration of the standard solution where primed quantities refer to the standard solution. Thus

$$\left(\frac{\sigma_K}{K}\right)^2 = \left(\frac{\sigma_S'}{S'}\right)^2 + \left(\frac{\sigma_L'}{L'}\right)^2$$

and therefore

$$\left(\frac{\sigma_S}{S}\right)^2 = \left(\frac{\sigma_S'}{S'}\right)^2 + \left(\frac{\sigma_L'}{L'}\right)^2 + \left(\frac{\sigma_L}{L}\right)^2 \quad \text{with } \sigma_L' = \sigma_L$$

The end points have generally been established within less than 0.001 inches on the micrometer and σ_L has been assumed to lie between 0.0005 and 0.0010 inches. A conservative estimate of σ_S' is 0.02 °/oo. For a typical calibration of a standard solution

$$S' = 16.03 \text{ °/oo}$$
$$L' = .4513 \text{ inches}$$
$$K = 35.32 \text{ °/oo/inch}$$

and for $\sigma_L' = 0.005$ inches and 0.0010 inches, the standard deviation of salinity, σ_S, is calculated to be 0.032 °/oo and 0.054 °/oo respectively. A value of $\sigma_S = \pm 0.04$ °/oo has been taken as representative of the error of the titrations.

Particular attention was taken in washing the sample vials and sampling equipment and the vials were tightly sealed with rubber stoppers when containing water samples. No attempts were made to control the temperature. The syringes were tested for constant displacement of fluid for equal displacements of the plungers and the errors resulting were found to be small compared to the other error sources. The difficulty in ascertaining the end point in the small volume of solution, approximately 2 cc, is believed to be the main source of error.

ACKNOWLEDGEMENTS

This work was supported by the National Science Foundation, Grants No. G 15728 and G 19788 and the Office of Naval Research, Contract Nonr-477(10), Project NR 083 012.

Table 1. Model Operating Conditions and Nondimensional Quantities M, F, and MF.

Run No.	Tide (Meters)	River Flow (m^3/sec)	M ($x10^7$)	F ($x10^{-3}$)	MF ($x10^4$)
1	3.54	1580	1.03	.50	.52
2	3.54	2820	.58	.90	.52
3	3.54	600	2.75	.19	.52
4	4.75	1580	1.39	.50	.70
5	4.75	2710	.81	.87	.50
6	4.75	510	4.28	.16	.69
7	2.44	1660	.68	.53	.36
8	2.44	2860	.39	.91	.35
9	2.44	550	2.04	.18	.36
10	2.44	1710	.66	.55	.36
12	3.54	2800	.58	.89	.52
14	6.30	2740	1.07	.87	.93
15	1.22	2700	.21	.86	.18
17	1.22	1630	.35	.52	.18
18	6.30	1550	1.88	.50	.94
19	1.22	600	.94	.19	.18
21	3.26	1580	.96	.50	.48
22	5.70	2650	1.00	.85	.85
23	6.30	1570	1.86	.50	.93
24	2.44	2610	.43	.83	.36

Table 2. Salinity-Depth Profile - Station: BUSH POINT

Salinity is in ratio $\frac{S_b - S_z}{S_o}$, Depth is in meters. The salinity ratio $\frac{S_o - S_b}{S_o}$ is indicated for each run (bottom line).

Depth \ Run	1a	1b	2a	2b	3a	3b	4a	4b	5a	5b
0	.011	.038	-	.066	.009	.006	.006	.012	.046	.052
10	-	-	-	-	-	-	-	-	-	-
25	.007	.002	-	.000	.004	.000	.000	.004	.006	.002
100	.000	.000	-	.000	.000	.000	.000	.000	.000	.000
$\frac{S_o - S_b}{S_o}$	.029	.028		.042	.006	.008	.026	.016	.025	.029

Depth \ Run	6a	6b	7a	7b	8a	8b	9a	9b	10a	10b
0	.001	.000	.116	.101	.328	.319	.016	.028	.095	.139
10	-	-	-	-	-	-	-	-	-	-
25	.001	.002	.010	.007	.016	.020	.006	.003	.003	.007
100	.000	.000	.000	.000	.000	.000	.000	.000	.000	.000
$\frac{S_o - S_b}{S_o}$	.006	.003	.029	.024	.045	.042	.007	.007	.026	.022

Depth \ Run	14a	14b	15a	15b	17a	17b	18a	18b	19a	19b	19c
0	.015	.020	.736	.740	.482	.516	.008	.010	.243	.231	.238
10	.002	.002	.057	.066	.048	.058	.002	.001	.023	.020	.020
25	.001	.002	.003	.009	.020	.020	.001	.002	.015	.014	.014
100	.000	.000	.000	.000	.000	.000	.000	.000	.000	.000	.000
$\frac{S_o - S_b}{S_o}$	.018	.017	.020	.018	.020	.018	.013	.013	.016	.014	.019

Depth \ Run	21a	21b	22a	22b	23a	23b	24a	24b
0	.085	.087	.039	.051	.011	.002	.411	.370
10	.010	.009	.006	.005	.002	.000	.024	.028
25	.006	.008	.004	.002	.001	.001	.015	.013
100	.000	.000	.000	.000	.000	.000	.000	.000
$\frac{S_o - S_b}{S_o}$	.021	.018	.023	.024	.008	.011	.032	.032

Table 3. Salinity-Depth Profile - Station: CAMANO HEAD

Salinity is in ratio $\frac{S_b - S_z}{S_o}$. Depth is in meters. The salinity ratio $\frac{S_o - S_b}{S_o}$ is indicated for each run (bottom line).

Depth \ Run	1a	1b	2a	2b	3a	3b	4a	4b	5a	5b
0	.62	.62	.77	.69	.29	.30	.52	.55	.76	.73
10	.019	.028	.035	.031	.015	.015	.018	.020	.035	.033
25	.007	.018	.027	.020	.008	.006	.010	.011	.015	.020
50	.008	.012	.012	.012	.005	.004	.006	.007	.011	.015
75	.007	.006	.007	.007	.003	.002	.002	.002	.007	.010
150	.000	.000	.000	.000	.000	.000	.000	.000	.000	.000
$\frac{S_o - S_b}{S_o}$	.046	.044	.077	.073	.029	.031	.045	.041	.055	.057

Depth \ Run	6a	6b	7a	7b	8a	8b	9a	9b	10a	10b
0	.18	.19	.64	.59	.68	.70	.34	.31	.68	.68
10	.023	.021	.042	.025	.053	.043	.019	.087	.021	.017
25	.008	.006	.011	.011	.007	.026	.010	.004	.009	.007
50	.007	.003	.009	.007	.004	.019	.007	.002	.007	.009
75	.003	.000	.007	.003	.007	.015	.002	.002	.002	.004
150	.000	.000	.000	.000	.000	.000	.000	.000	.000	.000
$\frac{S_o - S_b}{S_o}$	.015	.017	.046	.046	.069	.050	.028	.026	.045	.043

Depth \ Run	14a	14b	15a	15b	17a	17b	18a	18b	19a	19b	19c
0	.72	.63	.94	.96	.88	.87	.47	.46	.59	.58	.56
10	.060	.035	.17	.24	.16	.14	.005	.035	.090	.066	.068
25	.005	.008	.002	.010	.012	.012	.002	.008	.025	.011	.013
50	.004	.003	.000	.005	.011	.008	.002	.006	.018	.002	.007
75	.002	.002	.002	.004	.006	.002	.000	.000	.018	.000	.007
150	.000	.000	.000	.000	.000	.000	.000	.000	.000	.000	.000
$\frac{S_o - S_b}{S_o}$	.037	.036	.023	.018	.029	.028	.029	.029	-	.024	.022

Table 3 (continued). Salinity-Depth Profile - Station: CAMANO HEAD

Depth \ Run	21a	21b	22a	22b	23a	23b	24a	24b
0	.68	.72	.64	.72	.42	.43	-	.85
10	.029	.041	.021	.030	.021	.024	.040	.091
25	.012	.013	.006	.012	.006	.006	.015	.016
50	.009	.007	.004	.007	.005	.005	.014	.012
75	.009	.007	.002	.006	.004	.005	.011	.009
150	.000	.000	.000	.000	.000	.000	.000	.000
$\frac{S_o - S_b}{S_o}$	.036	.037	.049	.045	.024	.023	.046	.048

Table 4. Salinity-Depth Profile - Station: HAZEL POINT

Salinity is in ratio $\frac{S_b - S_z}{S_o}$. Depth is in meters. The salinity ratio $\frac{S_o - S_b}{S_o}$ is indicated for each run (bottom line).

Depth \ Run	1a	1b	2a	2b	3a	3b	4a	4b	5a	5b
0	.045	.046	.093	.084	.011	.017	.035	.022	.044	.048
10	[illegible]	[illegible]	[illegible]	[illegible]	[illegible]	[illegible]	[illegible]	[illegible]	[illegible]	[illegible]
25	.021	.022	.030	.034	.011	.010	.017	.009	.017	.017
100	.000	.000	.000	.000	.000	.000	.000	.000	.000	.000
$\frac{S_o - S_b}{S_o}$	.073	.066	.089	.090	.042	.043	.070	.074	.093	.097

Depth \ Run	6a	6b	7a	7b	8a	8b	9a	9b	10a	10b
0	.005	.003	.083	.083	.118	.112	.012	.021	.071	.075
10	-	-	-	-	-	-	-	-	-	-
25	.003	.000	.024	.027	.036	.035	.012	.018	.028	.030
100	.000	.000	.000	.000	.000	.000	.000	.000	.000	.000
$\frac{S_o - S_b}{S_o}$	.030	.031	.054	.050	.062	.062	.036	.030	.046	.044

Depth \ Run	12b	12c	12d	12e	14a	14b	15a	15b	17a	17b
0	.069	.071	.070	.075	.009	.005	.165	.111	.069	.066
10	.047	.049	.049	.054	.006	.000	.097	.104	.060	.058
25	.024	.024	.024	.024	.006	.000	.006	.009	.024	.025
100	.000	.000	.000	.000	.000	.000	.000	.000	.000	.000
$\frac{S_o - S_b}{S_o}$	.081	.080	.080	.087	.056	.062	.019	.017	.034	.029

Depth \ Run	18a	18b	19a	19b	19c	21a	21b	22a	22b
0	.011	.002	.030	.025	.025	.050	.047	.019	.021
10	.002	.000	.028	.023	.023	.034	.028	.002	.010
25	.001	.000	.026	.022	.024	.015	.010	.000	.006
100	.000	.000	.000	.000	.000	.000	.000	.000	.000
$\frac{S_o - S_b}{S_o}$	.047	.052	.025	.024	.028	.051	.050	.090	.079

Table 4 (continued). Salinity-Depth Profile - Station: HAZEL POINT

Depth \ Run	23a	23b	24a	24b
0	.004	.005	.098	.102
10	.000	.000	.071	.074
25	.000	.000	.010	.013
100'	.000	.000	.000	.000
$\frac{S_o - S_b}{S_o}$	.045	.044	.051	.050

Table 5. Salinity-Depth Profile — Station: POINT JEFFERSON

Salinity is in ratio $\frac{S_b - S_z}{S_o}$. Depth is in meters. The salinity ratio $\frac{S_o - S_b}{S_o}$ is indicated for each run (bottom line).

Depth \ Run	1a	1b	2a	2b	3a	3b	4a	4b	5a	5b
0	.070	.064	.135	.095	.016	.015	.036	.034	.085	.096
10	.025	.028	.043	.035	.016	.012	.020	.021	.030	.034
25	.019	.020	.038	.029	.013	.011	.022	.020	.022	.025
50	.017	.013	.020	.017	.011	-	.017	.013	.016	.020
75	.010	.011	.011	.010	.007	.006	.009	.006	.008	.009
150	.000	.000	.000	.000	.000	.000	.000	.000	.000	.000
$\frac{S_o - S_b}{S_o}$	.046	.042	.071	.072	.025	.027	.042	.042	.055	.057

Depth \ Run	6a	6b	7a	7b	8a	8b	9a	9b	10a	10b
0	.008	.010	.088	.071	.177	.208	.028	.025	.077	.060
10	.006	.007	.042	.027	.039	.042	.009	.016	.032	.025
25	.004	.007	.030	.017	.029	.029	.008	.011	.024	.015
50	.004	.006	.021	.007	.016	.015	.003	.008	.014	.005
75	.002	.005	.017	.002	.007	.007	.002	.004	.012	.006
150	.000	.000	.000	.000	.000	.000	.000	.000	.000	.000
$\frac{S_o - S_b}{S_o}$	.017	.015	.036	.047	.066	.059	.030	.024	.036	.040

Depth \ Run	12b	12c	12d	12e	14a	14b	15a	15b	17a	17b
0	.098	.089	.097	.099	.030	.035	.645	.695	.339	.345
10	.034	.032	.036	.035	.014	.016	.132	.142	.075	.079
25	.026	.025	.025	.026	.013	.009	.022	.030	.034	.027
50	.016	.017	.016	.017	.012	.007	.005	.005	.005	.007
75	.008	.007	.009	.007	.008	-	.000	.004	.004	.004
150	.000	.000	.000	.000	.000	.000	.000	.000	.000	.000
$\frac{S_o - S_b}{S_o}$	.063	.063	.063	.071	.037	.036	.021	.017	.029	.029

Table 5 (continued). Salinity-Depth Profile - Station: POINT JEFFERSON

Depth \ Run	18a	18b	19a	19b	19c	21a	21b	22a	22b
0	.015	.020	.102	.142	.139	.055	.050	.042	.052
10	.010	.011	.029	.029	.023	.023	.018	.021	.029
25	.007	.010	.015	.012	.011	.014	.011	.017	.025
50	.008	.008	.006	.002	.006	.011	.016	.014	.022
75	.005	.008	.004	.002	.002	.007	.007	.011	.016
150	.000	.000	.000	.000	.000	.000	.000	.000	.000
$\frac{S_o - S_b}{S_o}$	.029	.029	.025	.023	.026	.039	.041	.044	.037

Depth \ Run	23a	23b	24a	24b
0	.015	.014	-	.220
10	.011	.010	.034	.039
25	.010	.010	.025	.027
50	.008	.009	.009	.011
75	.006	.006	.005	.003
150	.000	.000	.000	.000
$\frac{S_o - S_b}{S_o}$	.026	.024	.051	.049

Table 6. Salinity-Depth Profile - Station: POINT PULLY

Salinity is in ratio $\frac{S_b - S_z}{S_o}$. Depth is in meters. The salinity ratio $\frac{S_o - S_b}{S_o}$ is indicated for each run (bottom line).

Depth \ Run	1a	1b	2a	2b	3a	3b	4a	4b	5a	5b
0	.020	.038	.031	.030	.014	.014	.014	.016	.020	.023
10	.019	.022	.027	.027	.014	.012	.012	.015	.019	.021
25	.020	.020	.025	.025	.012	.012	.012	.014	.017	.020
50	.017	.024	.023	.021	.010	.011	.013	.014	.016	.018
75	.012	.014	.005	.006	.010	.009	.011	.012	.014	.016
150	.000	.000	.000	.000	.000	.000	.000	.000	.000	.000
$\frac{S_o - S_b}{S_o}$	.051	.047	.079	.075	.029	.028	.046	.044	.059	.060

Depth \ Run	6a	6b	7a	7b	8a	8b	9a	9b	10a	10b
0	.007	.002	.028	.033	.051	.052	.016	.012	.026	.026
10	.005	.002	.023	.024	.028	.038	.016	.012	.023	.019
25	.006	.002	.020	.023	.030	.031	.012	.011	.020	.013
50	.004	.002	.012	.012	.016	.017	.010	.009	.011	.012
75	.004	.002	.004	.002	.002	.002	.005	.001	.002	.000
150	.000	.000	.000	.000	.000	.000	.000	.000	.000	.000
$\frac{S_o - S_b}{S_o}$	.020	.021	.049	.045	.061	.058	.029	.024	.049	.045

Depth \ Run	14a	14b	15a	15b	17a	17b	18a	18b	19a	19b	19c
0	.001	.008	.275	.282	.100	.107	.004	.003	.016	.020	.018
10	.005	.003	.089	.099	.049	.052	.002	.004	.016	.013	.017
25	.007	.005	.045	.049	.039	.032	.001	.006	.013	.014	.014
50	.004	.005	.004	.007	.006	.000	.003	.001	.013	.012	.009
75	.000	.003	.001	.003	.002	.001	.003	.003	.001	.002	.002
150	.000	.000	.000	.000	.000	.000	.000	.000	.000	.000	.000
$\frac{S_o - S_b}{S_o}$	.044	.042	.019	.017	.032	.028	.035	.037	.025	.024	.026

Table 6 (continued). Salinity-Depth Profile - Station: POINT PULLY

Depth \ Run	21a	21b	22a	22b	23a	23b	24a	24b
0	.017	.014	.016	.013	.001	.004	.048	.051
10	.013	.014	.014	.016	.002	.004	.032	.032
25	.015	.013	.012	.011	.001	.003	.031	.030
50	.016	.012	.014	.011	.000	.004	.021	.022
75	.007	.006	.009	-	.001	.003	.005	.006
150	.000	.000	.000	.000	.000	.000	.000	.000
$\frac{S_o - S_b}{S_o}$	.040	.040	.048	.048	.035	.030	.048	.049

Table 7. Salinity-Depth Profile - Station: SPRING BEACH

Salinity is in ratio $\frac{S_b - S_z}{S_o}$. Depth is in meters. The salinity ratio $\frac{S_o - S_b}{S_o}$ is indicated for each run (bottom line).

Depth \ Run	1a	1b	2a	2b	3a	3b	4a	4b	5a	5b
0	.003	.000	.010	.005	.001	.001	.002	.001	.000	.000
10	-	-	-	-	-	-	-	-	-	-
25	.002	.000	.004	.005	.000	.001	.002	.000	.000	.000
100	.000	.000	.000	.000	.000	.000	.000	.000	.000	.000
$\frac{S_o - S_b}{S_o}$	.066	.070	.100	.100	.044	.041	.064	.061	.081	.086

Depth \ Run	6a	6b	7a	7b	8a	8b	9a	9b	10a	10b
0	.000	.000	.007	.009	.027	.025	.002	.001	.009	.007
10	-	-	-	-	-	-	-	-	-	-
25	.000	.000	.003	.004	.012	.011	.003	.001	.007	.004
100	.000	.000	.000	.000	.000	.000	.000	.000	.000	.000
$\frac{S_o - S_b}{S_o}$	.028	.029	.067	.062	.086	.086	.040	.038	.060	.057

Depth \ Run	14a	14b	15a	15b	17a	17b	18a	18b	19a	19b	19c
0	.000	.000	.282	.311	.102	.116	.001	.000	.008	.010	.010
10	.001	.000	.048	.061	.042	.042	.000	.000	.007	.009	.009
25	.000	.000	.035	.039	.035	.033	.000	.001	.006	.007	.009
100	.000	.000	.000	.000	.000	.000	.000	.000	.000	.000	.000
$\frac{S_o - S_b}{S_o}$	.054	.053	.020	.016	.034	.032	.042	.045	.034	.032	.032

Depth \ Run	21a	21b	22a	22b	23a	23b	24a	24b
0	.003	.003	.001	.000	.000	.000	.019	.024
10	.002	.000	.001	.000	.001	.000	.013	.020
25	.003	.000	.000	.000	.001	.000	.011	.020
100	.000	.000	.000	.000	.000	.000	.000	.000
$\frac{S_o - S_b}{S_o}$	.054	.054	.067	.067	.039	.038	.067	.059

Table 8. Salinity-Depth Profile - Station: GORDON POINT

Salinity is in ratio $\frac{S_b - S_z}{S_o}$. Depth is in meters. The salinity ratio $\frac{S_o - S_z}{S_o}$ is indicated for each run (bottom line).

Depth \ Run	1a	1b	2a	2b	3a	3b	4b	5a	5b
0	.008	.002	.046	.033	.005	.005	.003	.020	.017
10	.005	.002	.009	.007	.003	.002	.002	.005	.008
25	.000	.002	.007	.007	.007	.002	-	.004	.007
50	.001	.002	.005	.003	.004	.002	.000	.002	.007
75	.000	.001	.001	.002	.002	.002	.001	.002	.005
150	.000	.000	.000	.000	.000	.000	.000	.000	.000
$\frac{S_o - S_b}{S_o}$	.078	.071	.106	.105	.042	.042	.062	.083	.085

Depth \ Run	6a	6b	7a	7b	8a	8b	9a	9b	10a	10b
0	.001	.000	.022	.029	.043	.034	.002	.000	.012	.016
10	.001	.000	.007	.006	.007	.007	.002	.002	.007	.007
25	.000	.005	.003	.005	.004	.004	.002	.002	.008	.008
50	.000	.001	.000	.002	.000	.002	.002	.000	.006	.002
75	.001	.000	.002	.000	.001	.004	.000	.000	.005	.001
150	.000	.000	.000	.000	.000	.000	.000	.000	.000	.000
$\frac{S_o - S_b}{S_o}$	.028	.030	.076	.075	.102	.097	.045	.038	.068	.068

Depth \ Run	12b	12c	12d	12e	14a	14b	15a	15b	17a	17b
0	.045	.028	.030	.030	.003	.006	.369	.354	.180	.203
10	.011	.011	.010	.010	.002	.004	.024	.030	.019	.016
25	.007	.009	.007	-	.002	.002	.016	.021	.007	.008
50	.005	.006	.005	-	.002	.002	.010	.017	.007	.007
75	.002	.003	.000	.003	.002	.001	.007	.010	-	.000
150	.000	.000	.000	.000	.000	.000	.000	.000	.000	.000
$\frac{S_o - S_b}{S_o}$	.094	.093	.095	.102	.054	.054	.050	.046	.066	.063

Table 8.(continued). Salinity-Depth Profile - Station: GORDON POINT

Depth \ Run	18a	18b	19a	19b	19c	21a	21b	22a	22b
0	.008	.011	.012	.014	.014	.007	.011	.007	.009
10	.002	.002	.008	.005	.009	.002	.002	.004	.001
25	.001	.002	.003	.005	.006	.002	.001	.003	.001
50	.000	.002	.000	.002	.002	.000	.005	.002	.001
75	.000	.003	.002	.002	.000	.005	.002	.000	.000
150	.000	.000	.000	.000	.000	.000	.000	.000	.000
$\frac{S_o - S_b}{S_o}$	.043	.043	.047	.044	.046	.059	.057	.066	.067

Depth \ Run	23a	23b	24a	24b
0	.007	.008	.027	.025
10	.004	.002	.011	.011
25	.002	.002	.007	.008
50	.003	.002	.002	.003
75	.003	.002	.002	.000
150	.000	.000	.000	.000
$\frac{S_o - S_b}{S_o}$	.037	.035	.084	.084

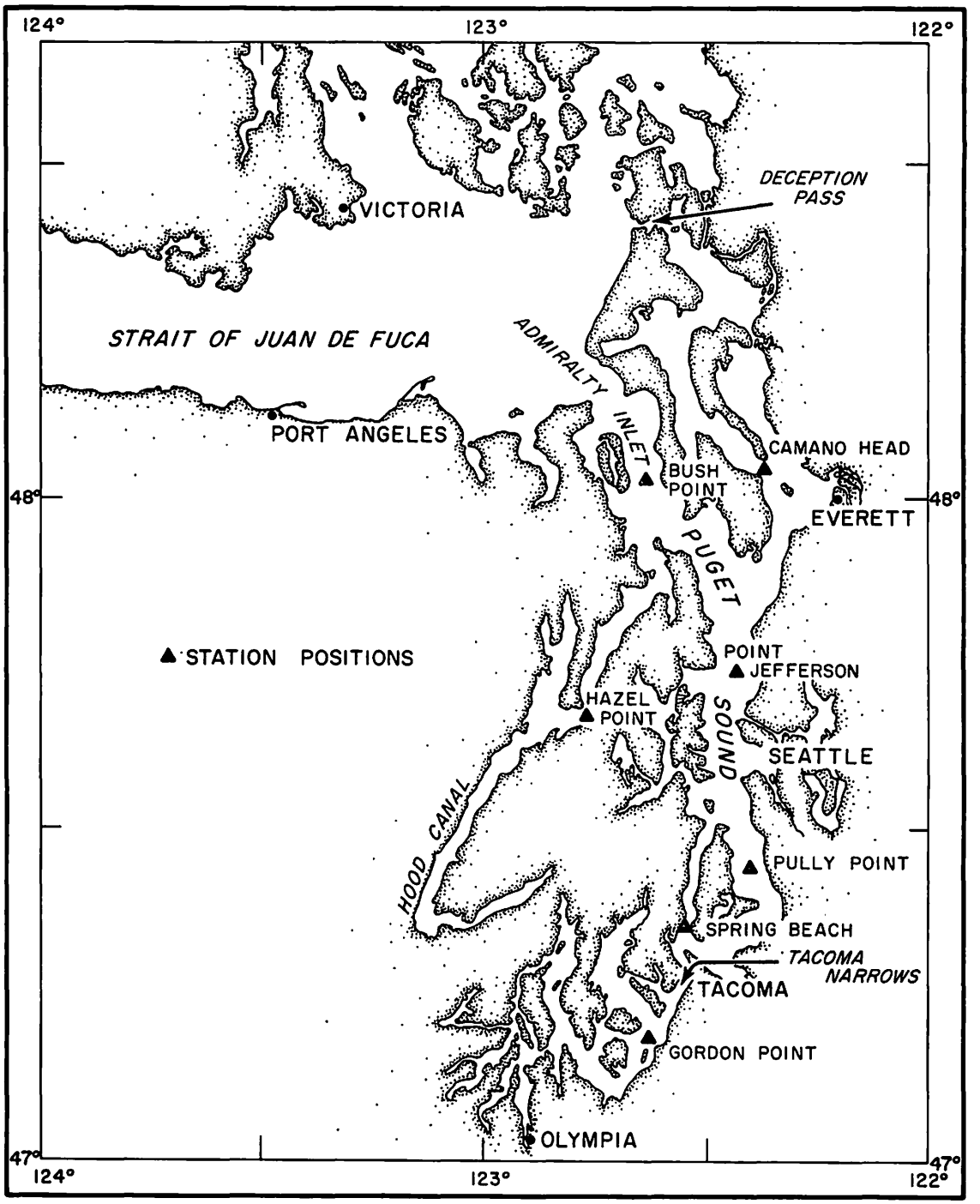

Fig. 1. Map of Puget Sound indicating station locations.

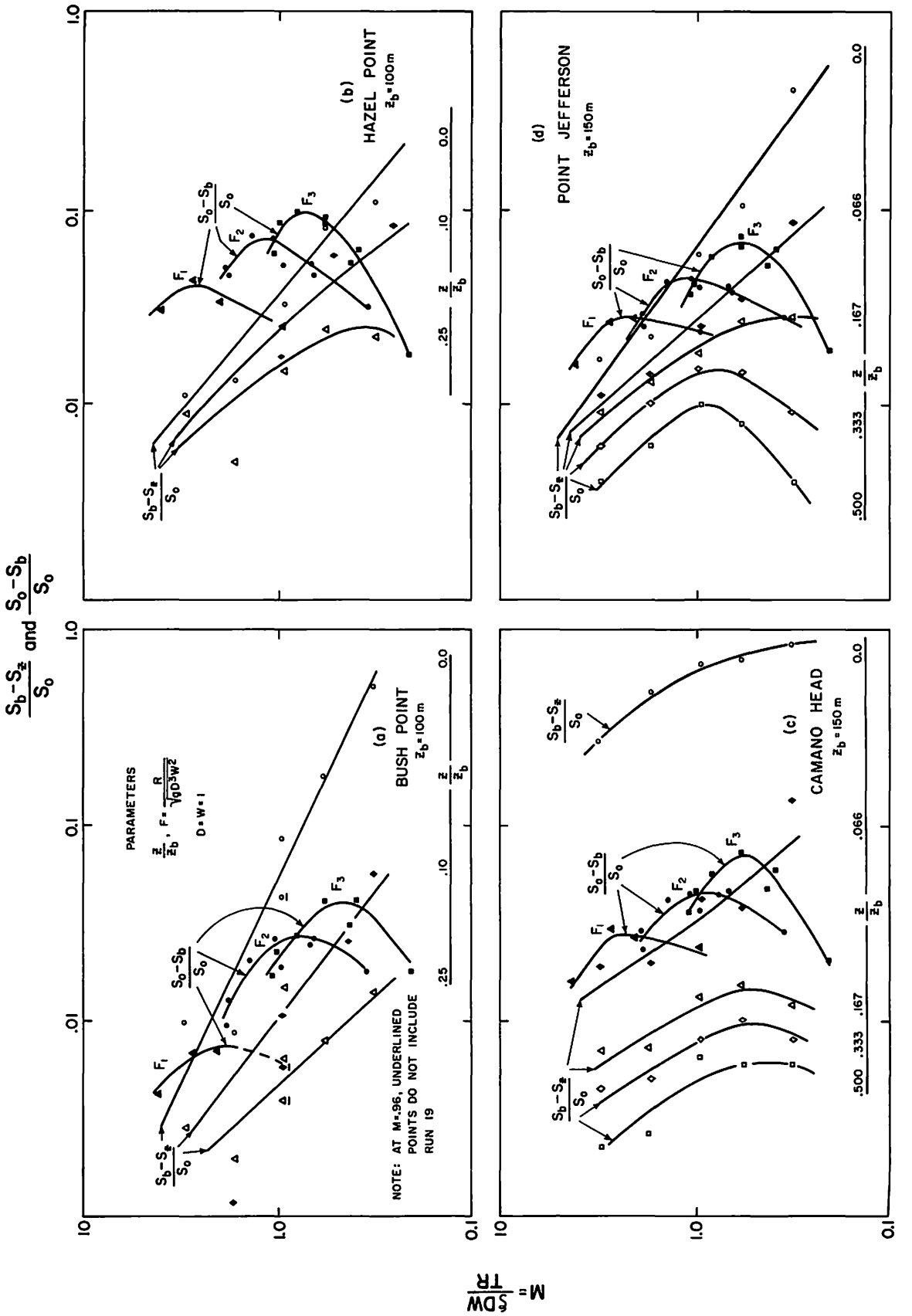

Fig. 2. (a,b,c,d) The salinity $\frac{S_b - S_z}{S_o}$ and $\frac{S_o - S_b}{S_o}$ versus the quantity $M = \frac{\zeta DW}{TR}$ with the parameter $\frac{z}{z_b}$.

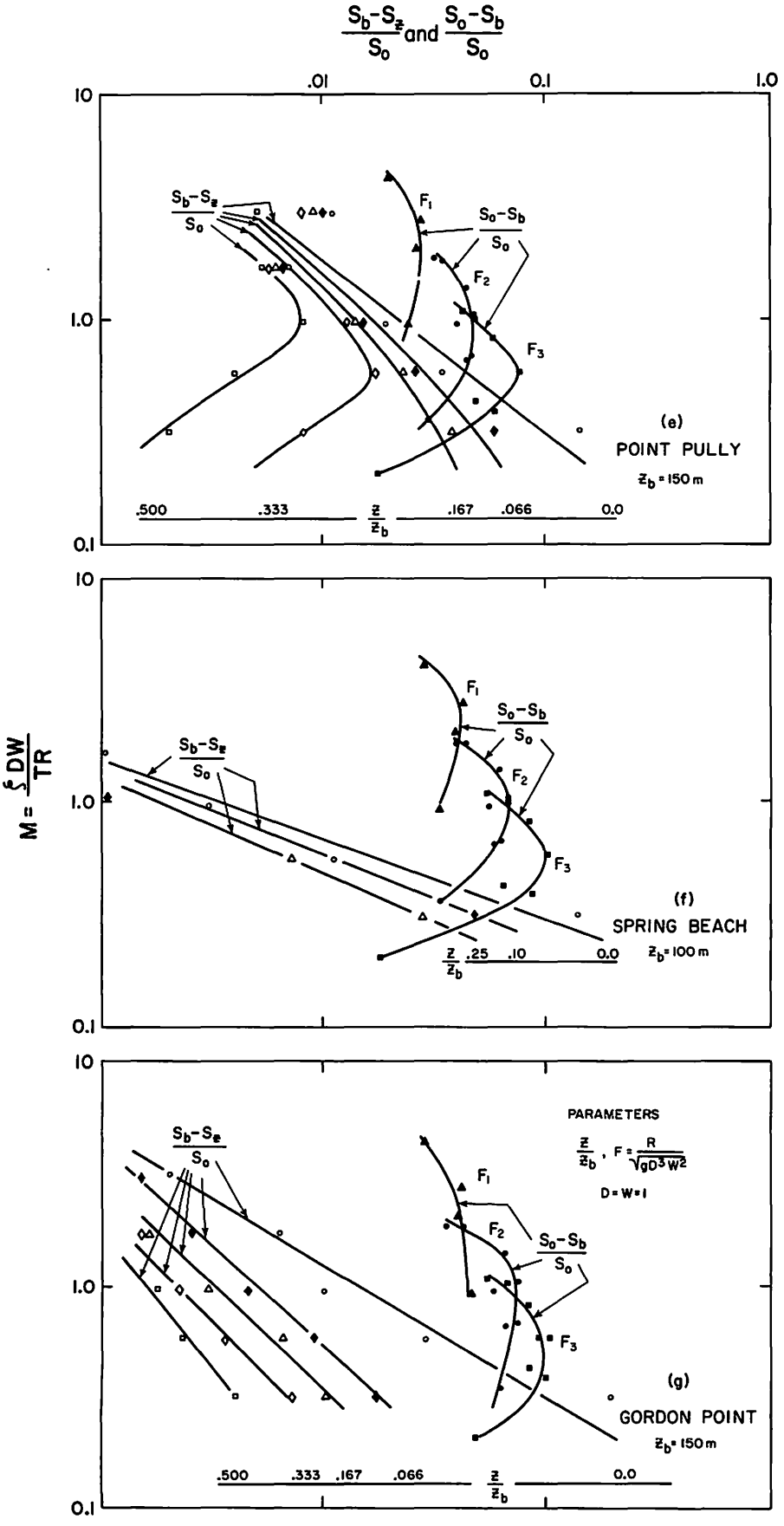

Fig. 2. (e,f,g) The salinity $\frac{S_b - S_z}{S_o}$ and $\frac{S_o - S_b}{S_o}$ versus the quantity $M = \frac{\int DW}{TR}$ with the parameter $\frac{z}{z_b}$.

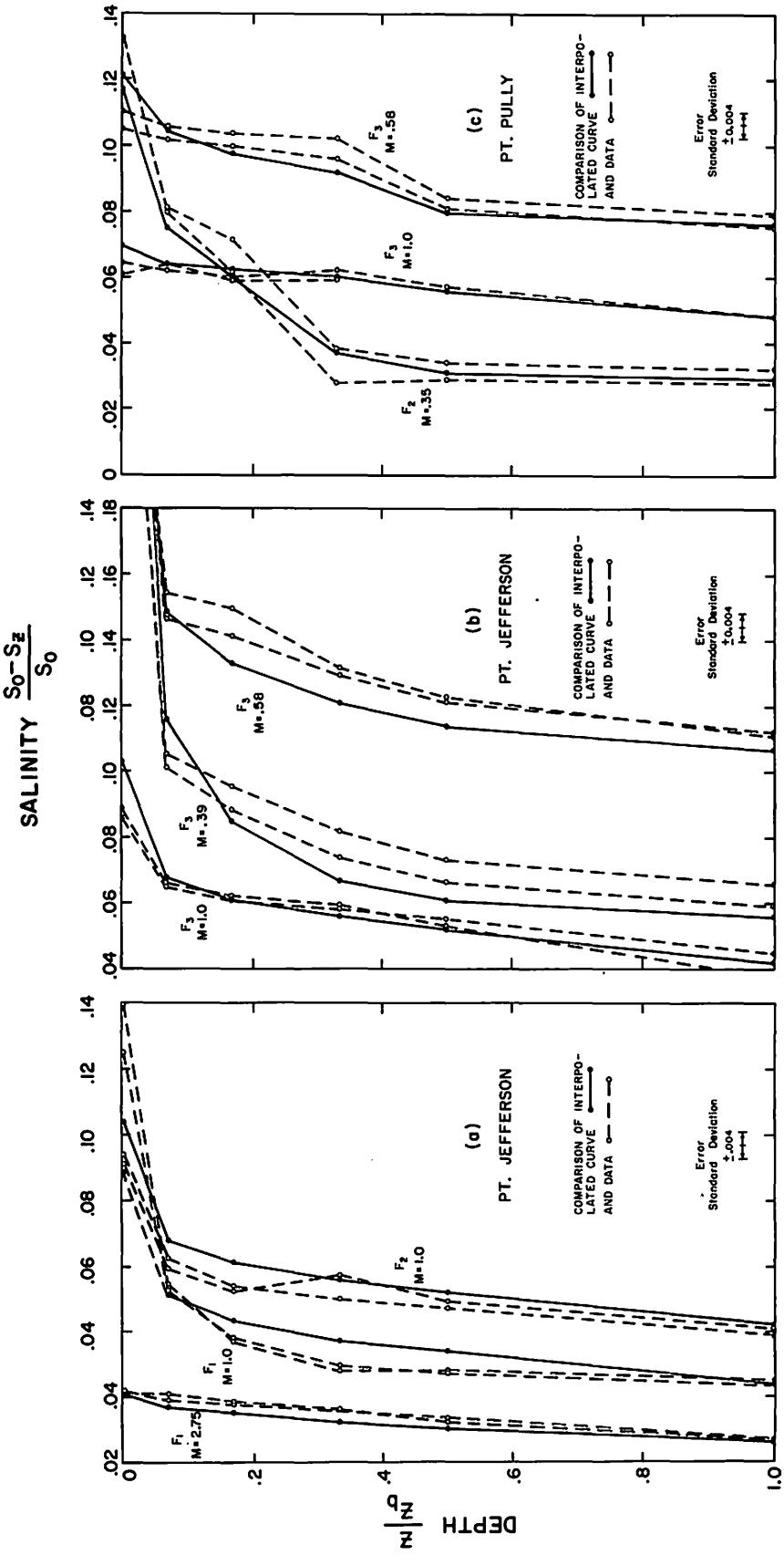

Fig. 3. The salinity profiles $\frac{S_o - S_z}{S_o}$ versus $\frac{z}{z_b}$ a comparison of interpolated profiles obtained from Fig. 2 with the original data for Point Pully and Point Jefferson.

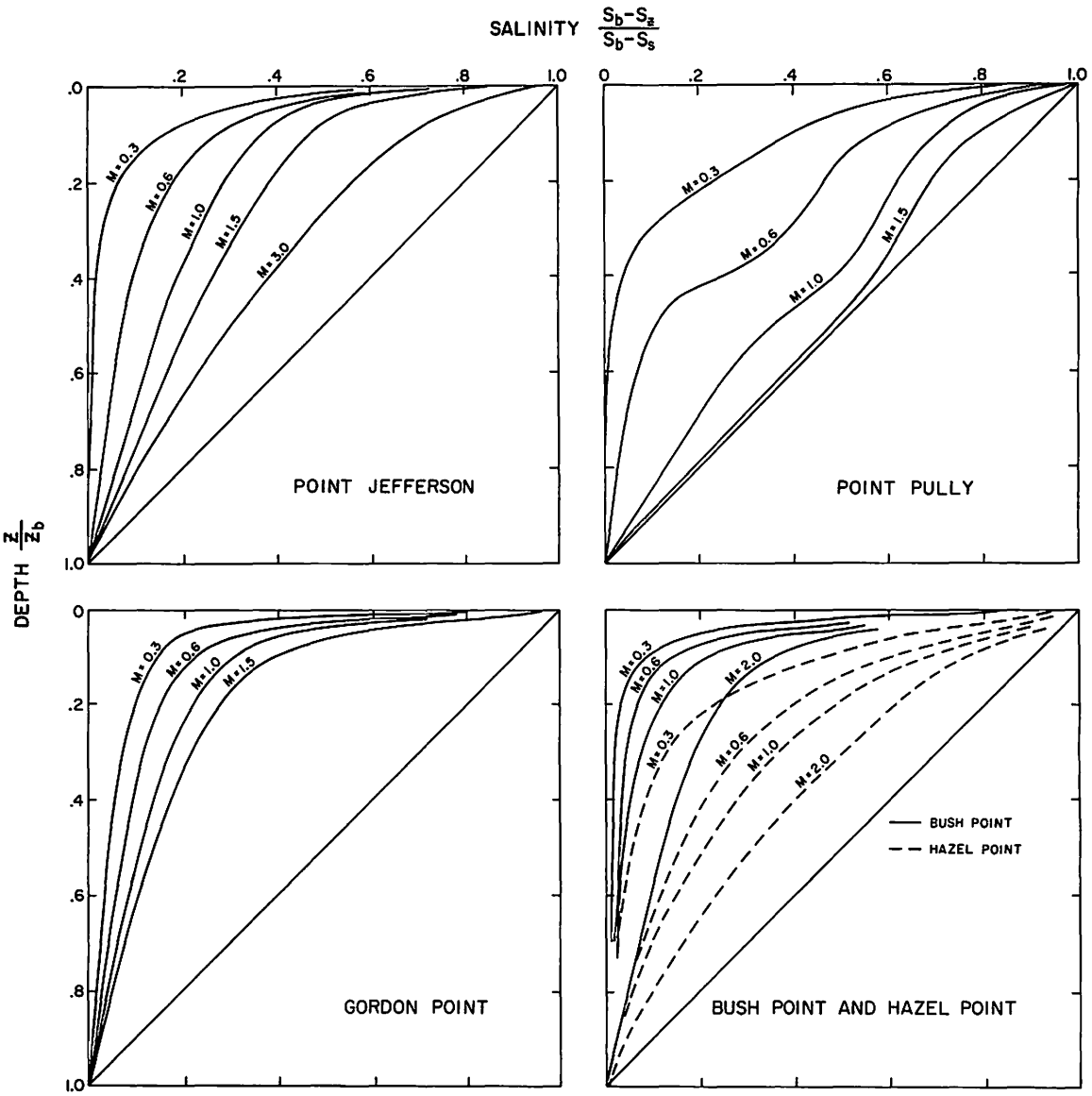

Fig. 4. Normalized salinity profiles $\frac{S_b - S_z}{S_b - S_s}$ versus $\frac{z}{z_b}$.

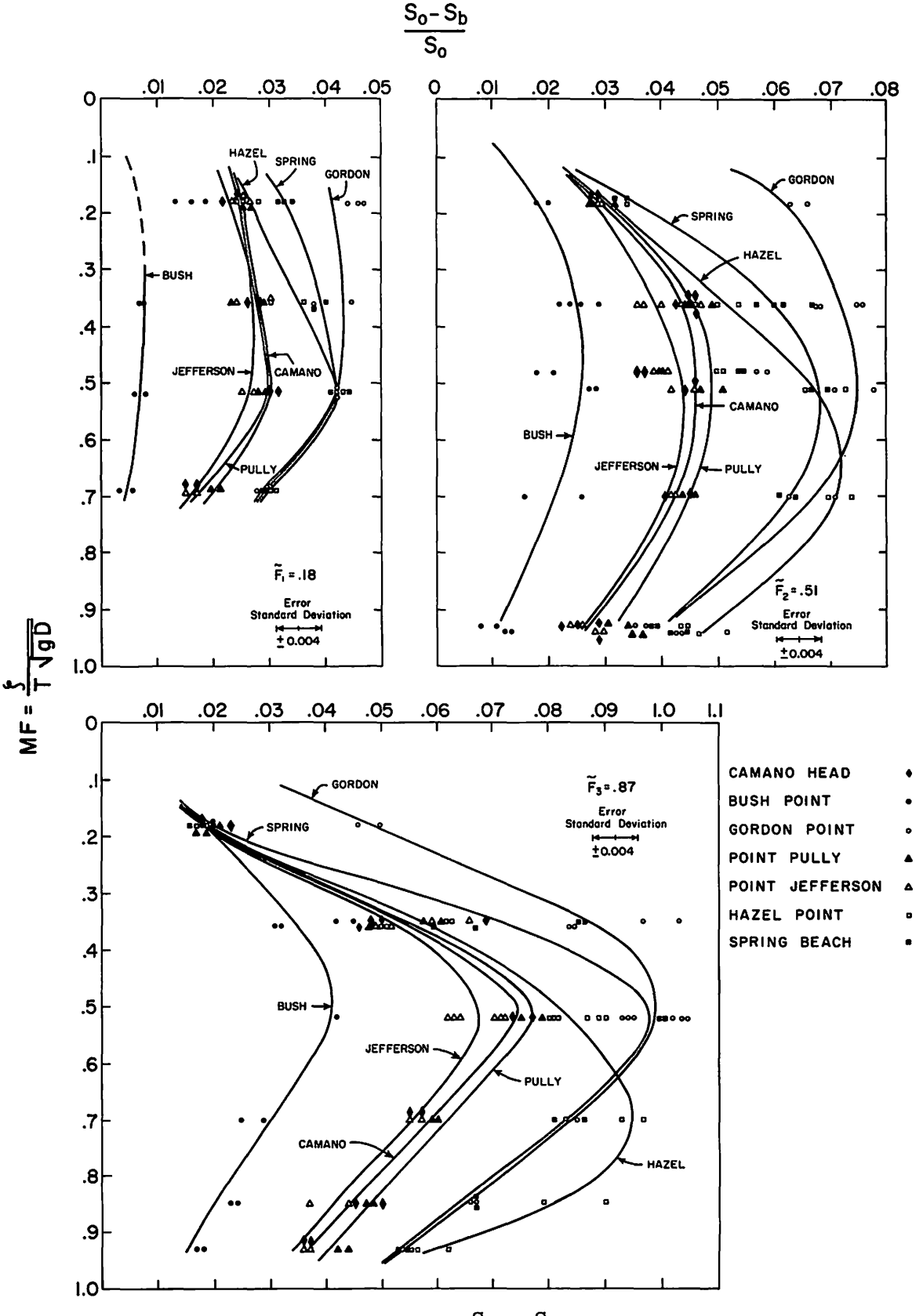

Fig. 5. Bottom salinity distribution $\frac{S_o - S_b}{S_o}$ versus MF = $\frac{\zeta}{T\sqrt{gD}}$ for the three conditions of runoff: low, F_1, mean, F_2, and high, F_3.

UNCLASSIFIED TECHNICAL REPORTS DISTRIBUTION LIST
for OCEANOGRAPHIC CONTRACTORS
of the GEOPHYSICS BRANCH
of the OFFICE OF NAVAL RESEARCH

DEPARTMENT OF DEFENSE

1 Director of Defense Research
& Engineering
Attn: Coordinating Committee
on Science
Pentagon
Washington 25, D. C.

NAVY

2 Office of Naval Research
Geophysics Branch (Code 416)
Washington 25, D. C.

Office of Naval Research
Washington 25, D. C.
1 Attn: Biology Branch (Code 446)
1 Attn: Surface Branch (Code 463)
1 Attn: Undersea Warfare (Code 466)
1 Attn: Special Projects (Code 418)

1 Commanding Officer
Office of Naval Research Branch
495 Summer Street
Boston 10, Massachusetts

1 Commanding Officer
Office of Naval Research
207 West 24th Street
New York 11, New York

1 Commanding Officer
Office of Naval Research Branch
The John Crearar Library Building
35 West 33rd Street
Chicago 16, Illinois

1 Commanding Officer
Office of Naval Research Branch
1000 Geary Street
San Francisco 9, California

1 Commanding Officer
U. S. Navy Mine Defense Laboratory
Panama City, Florida

NAVY

1 Commanding Officer
Office of Naval Research Branch
1030 East Green Street
Pasadena 1, California

10 Commanding Officer
Office of Naval Research Branch
Navy #100, Fleet Post Office
New York, New York

1 Contract Administrator Southeast Area
Office of Naval Research
2110 "G" Street, N. W.
Washington 7, D. C.

6 Director
Naval Research Laboratory
Attn: Technical Services
Information Officer
Washington 25, D. C.

(Note: 3 copies are forwarded by
this addressee to the British
Joint Services Staff for further
distribution in England and Canada)

8 Hydrographer
U. S. Navy Hydrographic Office
Washington 25, D. C.
Attn: Library (Code 1640)

1 U. S. Navy Branch
Hydrographic Office
Navy 3923, Box 77
F. P. O.
San Francisco, California

Chief, Bureau of Naval Weapons
Department of the Navy
Washington 25, D. C.
1 Attn: FASS
1 Attn: RU-222

1 Office of the U. S. Naval
Weather Service
U. S. Naval Station
Washington 25, D. C.

NAVY

1 Chief, Bureau of Yards & Docks
Office of Research
Department of the Navy
Washington 25, D. C.
Attn: Code 70

1 Commanding Officer & Director
U. S. Navy Electronics Laboratory
San Diego 52, California
1 Attn: Code 2201
1 Attn: Code 2420

1 Commanding Officer & Director
U. S. Naval Civil Engineering Laboratory
Port Hueneme, California
Attn: Code L54

1 Code 3145
Box 7
Pt. Mugu Missile Range
Pt. Mugu, California

1 Commander, Naval Ordnance Laboratory
White Oak, Silver Spring, Maryland
Attn: E. Liberman, Librarian

1 Commanding Officer
Naval Ordnance Test Station
China Lake, California
1 Attn: Code 753
1 Attn: Code 508

1 Commanding Officer
Naval Radiological Defense Laboratory
San Francisco, California

Chief, Bureau of Ships
Department of the Navy
Washington 25, D. C.
1 Attn: Code 312
1 Attn: Code 341C
1 Attn: Code 631
1 Attn: Code 688

1 Commanding Officer
U. S. Navy Mine Defense Laboratory
Panama City, Florida

1 Officer in Charge
U. S. Navy Weather Research Facility
Naval Air Station, Bldg. R-48
Norfolk, Virginia

1 Commanding Officer
U. S. Navy Air Development Center
Johnsville, Pennsylvania
Attn: NADC Library

1 Superintendent
U. S. Naval Academy
Annapolis, Maryland

2 Department of Meteorology & Oceanography
U. S. Naval Postgraduate School
Monterey, California

1 Commanding Officer
U. S. Naval Underwater Sound Laboratory
New London, Connecticut

1 Commanding Officer
U. S. Naval Underwater Ordnance Station
Newport, R. D./Ad3 (WS.D.) wsd. 5600/1

AIR FORCE

1 Hdqtrs., Air Weather Service
(AWSS/TIPD)
U. S. Air Force
Scott Air Force Base, Illinois

1 AFCRL (CRZF)
L. G. Hanscom Field
Bedford, Massachusetts

ARMY

1 Army Research Office
Office of the Chief of R&D
Department of the Army
Washington 25, D. C.

1 U. S. Army Beach Erosion Board
5201 Little Falls Road, N. W.
Washington 16, D. C.

1 Director
U. S. Army Engineers Waterways Experiment Station
Vicksburg, Mississippi
Attn: Research Center Library

1 Laboratory Director
Bureau of Commercial Fisheries
Biological Laboratory
Bldg. 74, Wash. Navy Yard Annex
Washington 25, D. C.

ARMY

1 Laboratory Director
Bureau of Commercial Fisheries
Biological Laboratory
450-B Jordan Hall
Stanford, California

Bureau of Commercial Fisheries
U. S. Fish & Wildlife Service
Post Office Box 3830
Honolulu 12, Hawaii
1 Attn: Librarian

1 Director
National Oceanographic Data Center
Washington 25, D. C.

OTHER U. S. GOVERNMENT AGENCIES

1 Office of Technical Services
Department of Commerce
Washington 25, D. C.

10 Armed Services Technical
Information Agency
Arlington Hall Station
Arlington 12, Virginia

2 National Research Council
2101 Constitution Avenue
Washington 25, D. C.
Attn: Committee on Undersea Warfare
Attn: Committee on Oceanography

1 Commanding Officer
U. S. Coast Guard Oceanographic Unit
c/o Woods Hole Oceanographic Inst.
Woods Hole, Massachusetts

1 Commandant (OFU)
U. S. Coast Guard
Washington 25, D. C.

1 Director
Coast & Geodetic Survey
U. S. Department of Commerce
Washington 25, D. C.
Attn: Office of Oceanography

1 U. S. Geological Survey
Washington 25, D. C.
Attn: James Trumbull

1 Director of Meteorological Research
U. S. Weather Bureau
Washington 25, D. C.

2 Library, U. S. Weather Bureau
Washington 25, D. C.

2 Director, Bureau of
Commercial Fisheries
U. S. Fish & Wildlife Service
Department of Interior
Washington 25, D. C.

1 U. S. Bureau of Commercial Fisheries
Fish & Wildlife Service
P. O. Box 271
La Jolla, California

RESEARCH LABORATORIES

2 Director
Woods Hole Oceanographic Institution
Woods Hole, Massachusetts

3 Project Officer
Laboratory of Oceanography
Woods Hole, Massachusetts

1 Director
Narragansett Marine Laboratory
University of Rhode Island
Kingston, Rhode Island

1 Bingham Oceanographic Laboratories
Yale University
New Haven, Connecticut

Gulf Coast Research Laboratory
Post Office Box
Ocean Springs, Mississippi
Attn: Librarian

1 Chairman
Department of Meteorology &
Oceanography
New York University
New York 53, New York

1 Director
Lamont Geological Observatory
Torrey Cliff
Palisades, New York

1 Director
Hudson Laboratories
145 Palisades Street
Dobbs Ferry, New York

RESEARCH LABORATORIES

1 Great Lakes Research Division
Institute of Science & Technology
University of Michigan
Ann Arbor, Michigan
1 Attn: Dr. John C. Ayers

1 Dr. Harold Haskins
Rutgers University
New Brunswick, New Jersey

1 Director
Chesapeake Bay Institute
Johns Hopkins University
121 Maryland Hall
Baltimore 18, Maryland

1 Mail No. J-3009
The Martin Company
Baltimore 3, Maryland
Attn: J. D. Pierson

1 Mr. Henry D. Simmons, Chief
Estuaries Section
Waterways Experiment Station
Corps of Engineers
Vicksburg, Mississippi

1 Oceanographic Institute
Florida State University
Tallahassee, Florida

1 Director, Marine Laboratory
University of Miami
#1 Rickenbacker Causeway
Virginia Key
Miami 49, Florida

1 Nestor C. L. Granelli
Department of Geology
Columbia University
Palisades, New York

2 Head, Department of Oceanography
and Meteorology
Texas A & M College
College Station, Texas

1 Director
Scripps Institution of Oceanography
La Jolla, California

1 Allan Hancock Foundation
University Park
Los Angeles 7, California

1 Department of Engineering
University of California
Berkeley, California

1 Head, Department of Oceanography
Oregon State University
Corvallis, Oregon

1 Director
Arctic Research Laboratory
Barrow, Alaska

1 Dr. C. I. Beard
Boeing Scientific Research Laboratories
P. O. Box 3981
Seattle 24, Washington

1 Head, Department of Oceanography
University of Washington
Seattle 5, Washington

1 Geophysical Institute of the
University of Alaska
College, Alaska

1 Director
Bermuda Biological Station
for Research
St. Georges, Bermuda

1 Department of Meteorology
and Oceanography
University of Hawaii
Honolulu 14, Hawaii
Attn: Dr. H. M. Johnson

1 Technical Information Center, CU-201
Lockheed Missile and Space Division
3251 Hanover Street
Palo Alto, California

1 Stanford Research Institute
Department of Earth Sciences
Menlo Park, California

RESEARCH LABORATORIES

1 University of Pittsburgh
Environmental Sanitation
Department of Public Health Practice
Graduate School of Public Health
Pittsburgh 13, Pennsylvania

1 Director
Hawaiian Marine Laboratory
University of Hawaii
Honolulu, Hawaii

1 Dr. F. B. Berger
General Precision Laboratory
Pleasantville, New York

1 Dr. J. A. Gast
Oceanography
Humboldt State College
Arcata, California

1 Department of Geodesy & Geophysics
Cambridge University
Cambridge, England

1 Applied Physics Laboratory
University of Washington
1013 NE Fortieth Street
Seattle 5, Washington

1 Documents Division - ml
University of Illinois Library
Urbana, Illinois

1 Laboratory Director
Biological Laboratory
Bureau of Commercial Fisheries
Building 74, Naval Weapons Plant
Washington 25, D. C.

1 Advanced Research Projects Agency
Attn: Nuclear Test Detection Office
The Pentagon
Washington 25, D. C.

1 New Zealand Oceanographic Institute
Department of Scientific and
Industrial Research
P. O. Box 8009
Wellington, New Zealand
Attn: Librarian

1 President
Osservatorio Geofisico Sperimentale
Trieste

1 Advanced Undersea Warfare
Engineering
Advanced Electronics Center
General Electric Company
Ithaca, New York